The Astrophysical Journal, 778:25 (7pp), 2013 November 20 doi:10.1088/0004-637X/778/1/25

SHORT-SCALE VARIATIONS OF THE SOLAR WIND HELIUM ABUNDANCE

J. Šafránková[1], Z. Němeček[1], P. Cagaš[1], L. Přech[1], J. Pavlů[1], G. N. Zastenker[2], M. O. Riazantseva[2], and I. V. Koloskova[2]
[1] Faculty of Mathematics and Physics, Charles University, V Holešovičkách 2, 18000 Prague 8, Czech Republic; jana.safrankova@mff.cuni.cz
[2] Space Research Institute of Russian Academy of Sciences, Profsoyuznaya ul. 84/32, Moscow 117997, Russia
Received 2013 August 7; accepted 2013 September 20; published 2013 October 30

ABSTRACT

Abrupt changes of the relative He abundance in the solar wind are usually attributed to encounters with boundaries dividing solar wind streams from different sources in the solar corona. This paper presents a systematic study of fast variations of the He abundance that supports the idea that a majority of these variations on short timescales (3–30 s) are generated by in-transit turbulence that is probably driven by the speed difference between the ion species. This turbulence contributes to the solar wind heating and leads to a correlation of the temperature with He abundance.

Key word: solar wind

Online-only material: color figures

1. INTRODUCTION

Helium plays a significant role in the structure and dynamics of the solar corona and solar wind. It is an important parameter that is often used for the determination of an origin of solar wind structures, such as the streamers extending into the heliospheric current sheet (e.g., Borrini et al. 1981; Kasper et al. 2008). Variations of the relative abundance of helium to hydrogen defined as $A_{\rm He} = 100 \times (n_{\rm He}/n_{\rm H})$ have been reported by many authors. $A_{\rm He}$ is generally steady and close to 5% in high-speed streams (Bame et al. 1977), whereas it tends to be lower and more variable in the slow solar wind.

Aellig et al. (2001) found a clear dependence of the He/H ratio on the solar cycle in agreement with previous papers (Ogilvie & Hirshberg 1974; Feldman et al. 1978; Neugebauer 1981; Ogilvie et al. 1989). In studies based on *Wind* spacecraft data, Kasper et al. (2007) and Richardson & Kasper (2008) have shown that a highly averaged (250 days) $A_{\rm He}$ in the slow solar wind ($v < 420$ km) is correlated with the sunspot number and ranges between 1% and 4%, whereas $A_{\rm He}$ is nearly constant and equal to ≈4% in the high-speed solar wind. Furthermore, the authors found $A_{\rm He}$ to be a rising function of the solar wind speed, but this dependence is very weak during solar maximum. Their histograms of $A_{\rm He}$ in the low-speed solar wind (300–325 km s^{-1}) exhibit two peaks (at 1% and at 3%–4%) and $A_{\rm He}$ fluctuations with the solar cycle are connected with the variable proportion between these two peaks; the 1% peak is dominant during the solar minimum but it nearly disappears during the solar maximum. The authors suggest that the slow solar wind has two sources in the equatorial plane: one associated with the streamer belt dominates at the solar minimum and another that is strongly correlated with the number of active regions at lower latitudes prevails at the solar maximum.

The slow wind associated with open field regions is of two different types: one component originates from small coronal holes located in and around active regions, while the other component originates from just inside the boundaries of the large polar holes. On the other hand, superposed epoch plots of Borrini et al. (1981) based on hourly averaged data have revealed a factor of two depression of the He/H flux ratio near the heliospheric current sheet even if the current sheet crossings were not associated with the stream boundaries. The depression was accompanied by decreases of the proton temperature and speed.

Wang (2008) tried to relate the long-term changes of $A_{\rm He}$ to the magnetic field strength at source regions in the outer solar corona. $A_{\rm He}$ tends to be enhanced in high-speed flows and in the slow solar wind at sunspot maximum but to be weak in the low-speed wind that originates from the polar coronal hole boundaries around sunspot minimum. Wang (2008) attributed these $A_{\rm He}$ variations to different velocities of He and H and argues that $A_{\rm He} \sim n_p v_p$ at the source surface. Nevertheless, the correlation between $A_{\rm He}$ and the magnetic field at the source surface was found to be weak and seen only in the low-speed solar wind.

Viall et al. (2009) analyzed observations of a periodic structure in the solar wind where the H and He densities varied in anti-phase. The authors concluded that the observed ∼30 minute periodicity is most likely connected with temporal or spatial variations of the source in the solar corona.

Borovsky (2008) argued that the inner heliosphere is filled with magnetic field tubes that are fossil structures that originated at the solar surface. The tube wall crossings are associated with large changes in the magnetic field direction, vector flow velocity, ion entropy density, and the He/H flux ratio. The median size of the flux tubes at 1 AU is 4.4×10^5 km.

The analysis of *Ulysses* and *Helios* data (Neugebauer et al. 1996) has shown that the velocities of H and He can differ but the difference seems to be limited by the Alfvén speed. The mean difference is about 30 km s^{-1} at 1 AU and decreases with a solar wind travel time. According to Steinberg et al. (1996), this difference increases with the solar wind speed but the effect is small at 1 AU. Marsch et al. (1982) discussed the radial dependence of the He/H differential flow speed. From their Figure 10, it follows that the difference between He and H velocities is very small for the slow solar wind (<400 km s^{-1}) and it undergoes a negligible evolution along the path from 0.3 to 1 AU. On the other hand, it can be as large as 150 km s^{-1} at 0.3 AU in the fast solar wind (>500 km s^{-1}) and rapidly decreases to ≈40 km s^{-1} near Earth's orbit.

From this short survey, it follows that the main attention was focused on long-term $A_{\rm He}$ variations; only a small portion of studies discuss very quick and strong variations on a short scale. Based on fast measurements on the *Prognoz* 7, 8, and

9 spacecraft, Avanov et al. (1987) and Yermolaev & Stupin (1997) explained different behaviors of the helium abundance in heliospheric current sheets, in coronal streamers, and in coronal holes. Owens et al. (2011) analyzed interplanetary magnetic field (IMF) discontinuities and their relation to jumps of other parameters including A_{He} on a scale of ≈1 minute. The authors found that large changes of the IMF magnitude and/or IMF rotations over a large angle are accompanied by significant jumps of the velocity ≈85% of the time but only about ≈25% of the time by A_{He} jumps. They concluded that this difference is connected with the sources of the observed jumps; while the jump of A_{He} is caused exclusively by the crossing of a boundary dividing two solar wind streams emanating from different source regions, many discontinuities in other parameters can originate on the path from the Sun due to in-transit turbulence. The experimental evidence supporting this conclusion is indirect and the study leaves many important questions regarding variations of A_{He} unanswered. We list only a few of them. How fast and how frequent are these changes of A_{He}? Are all significant A_{He} jumps connected with changes of the source region? Can the turbulence of the multi-component solar wind lead to a creation of fast variations of A_{He}? We present a study of fast variations of A_{He} with motivation to answer some of these questions.

2. USED EXPERIMENTAL DATA

This study uses measurements of the ion energy spectra by a set of Faraday cups (FCs) of the Bright Monitor of the Solar Wind (BMSW) instrument on board the *Spektr-R* project. The orbital parameters are appropriate for solar wind monitoring because the period is ≈8.2 days, apogee—333 570 km, and perigee—576 km. The spacecraft is usually located in the solar wind for ≈7–8 days per orbit. BMSW was designed predominantly for very fast measurements with a time resolution ranging from seconds to 31 ms. It works in two basic configurations with different time resolutions with sweeping and adaptive modes which are each used over parts of the orbit. A_{He} is reliably determined in the sweeping mode that provides a one-dimensional distribution function of solar wind ions and a direction of the velocity with a time resolution up to 1.5 s. The instrument itself and methods of data processing are described in Šafránková et al. (2013a, 2013b, 2013c), and thus we will describe only briefly the method of the A_{He} determination used in this paper.

Figure 1 shows the FC current as a function of the voltage applied on the control grid, HV. The current is normalized to the value corresponding to HV = 0 and is composed of the contributions of all ion species. The increasing voltage decelerates protons first and their contribution becomes negligible above about 800 V in this particular case. A plateau between ≈800 and 1000 V can be attributed to the contribution of alpha particles and other heavier species. We neglect the heavy ions and suppose that the FC current at HV = 0 is proportional to a sum of the proton flux and the flux of alpha particles multiplied by their charges, whereas the current corresponding to the plateau is due to the presence of alpha particles. The A_{He} ratio is computed from these two currents. We note that A_{He} computed in this way represents a ratio of the fluxes of these two species rather than the ratio of their densities, as is usually analyzed in previous studies.

Another important note is that although the energy spectra in Figure 1 were measured only 20 minutes apart, normalized alpha currents differ by an order of magnitude. In spite of a low contribution of alpha particles to the total current (≈1%) in the blue spectrum, this contribution can be undoubtedly resolved because the currents of heavier species and the instrumental noise are another order of magnitude lower (Šafránková et al. 2013c).

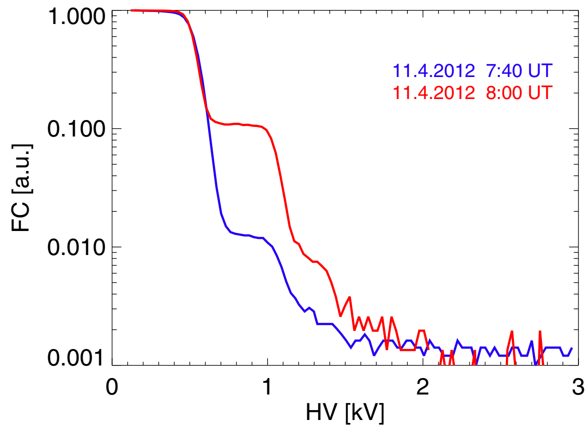

Figure 1. FC current as a function of the control grid voltage in two times. (A color version of this figure is available in the online journal.)

Finally, we also note three limitations of the experiment. (1) The voltages applied to the detector grids allow us a reliable A_{He} determination only for low and moderate speeds (up to ≈600 km s^{-1}). (2) The throughput of the spacecraft telemetry channel is not sufficient and thus only some of the data stored on board can be transmitted to the Earth. (3) The on board magnetometer is not in operation.

The analyzed data cover 180 hr of measurements from 2011 August to 2012 September and we are forced to use a propagated IMF from other spacecrafts; *Wind* data are used in this paper.

3. DATA ANALYSIS

The whole data set is presented in Figure 2 as two-dimensional probability histograms of observations of a particular A_{He} value under given conditions. The first panel shows a large variability of A_{He} (≈0%–12%) which rises with the solar wind speed on average. This rise is a consequence of an increasing probability of observations of larger A_{He} with faster solar wind speed, nevertheless, values around 2% are still frequent at the upper end of our speed range. The second panel displays a slightly enhanced A_{He} for dense ($n > 20$ cm^{-3}) solar wind that can be connected with the dependence of A_{He} (Wang 2008) on the proton flux at the source region. Nevertheless, the panel reveals a distinct group of observations of the dense solar wind (above 20 cm^{-3}) with a very low A_{He} (<1%). Comparison with the first panel shows that these low A_{He} values were observed at very low speeds, and thus the Wang (2008) suggestion probably holds even for these events.

The third panel shows the A_{He} rise with the proton thermal speed. This plot exhibits a rather good organization, suggesting either that the source of hotter solar wind lies deeper in the solar corona or that additional heating of the He occurs in the enriched solar wind stream.

The changes of A_{He} are not smooth. The spacecraft often observed abrupt transitions from one state to another, as Figure 3(a) demonstrates. The top panel shows the ion energy spectrogram where two distinct lines can be clearly identified. The lower line (at ≈500 eV) belongs to protons, whereas the upper line represents the helium differential energy flux. A comparison of

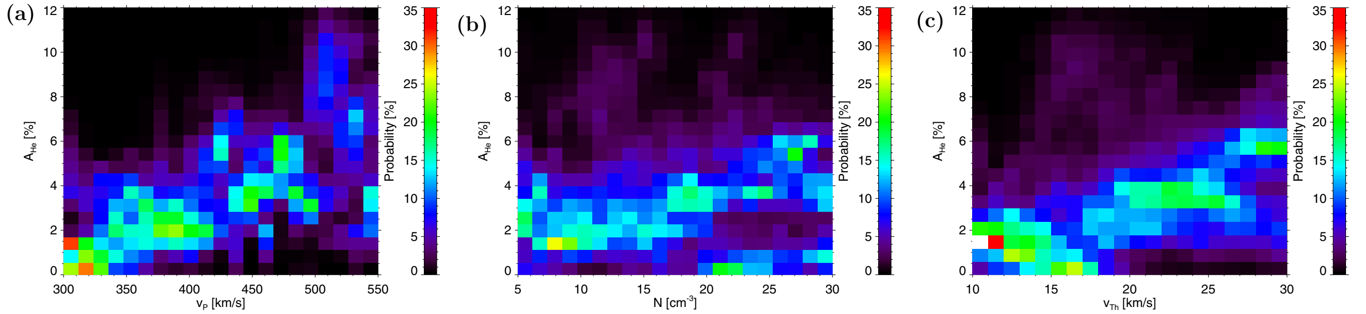

Figure 2. Two-dimensional probability histograms of observations of A_{He} as a function of the proton bulk speed (a); proton density (b); and proton thermal speed (c). The color scale presents a number of events in a particular bin normalized to the total number of counts in the corresponding column.

(A color version of this figure is available in the online journal.)

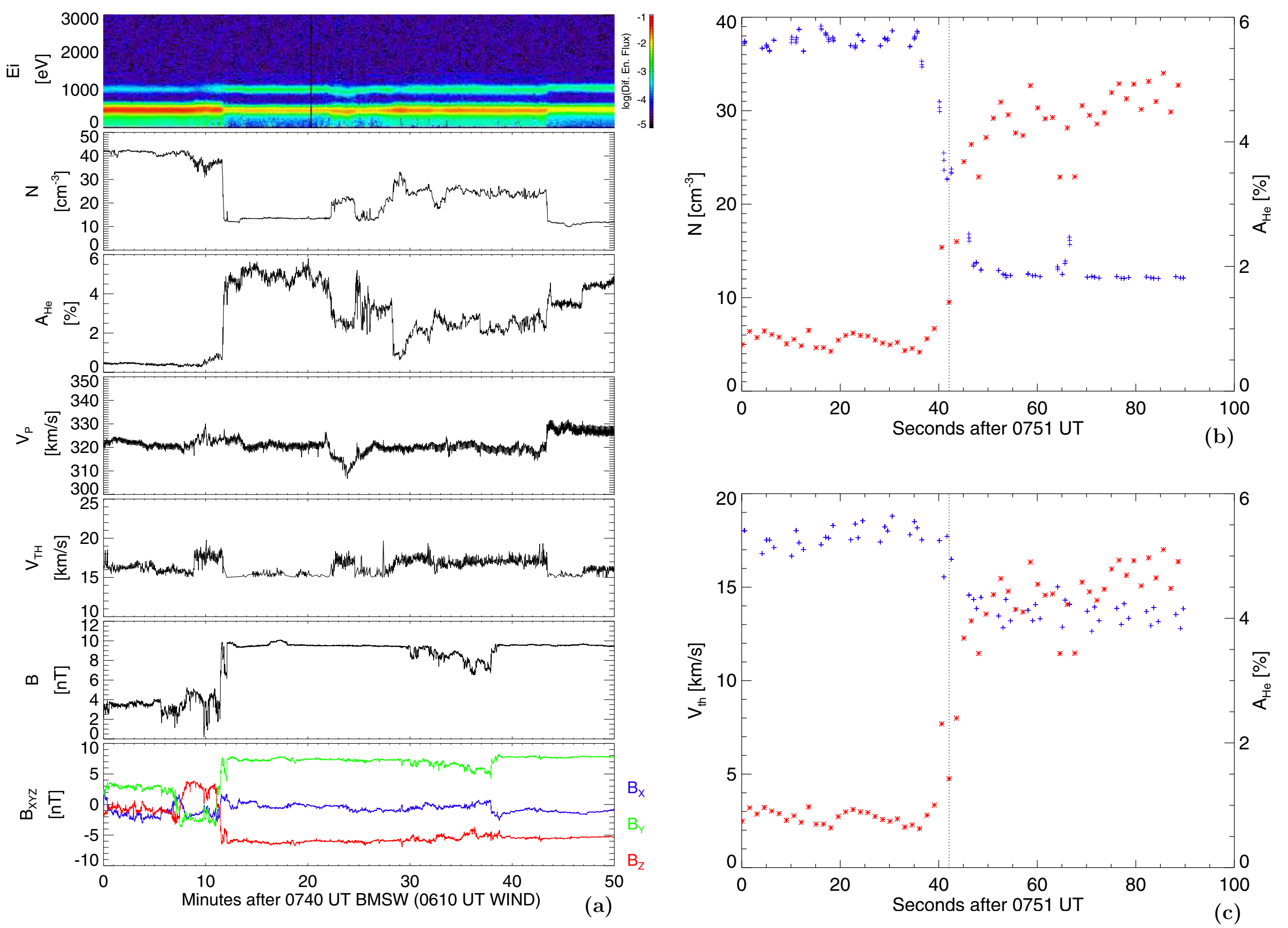

Figure 3. Example of fast fluctuations of the He/H ratio. (a) The overview of the *Spektr-R* and *Wind* observations on 2012 April 11, after 0740 UT. From top to bottom: ion energy spectrogram; the proton density; A_{He}; proton bulk and thermal velocities (from *Spektr-R*) and the magnitude and all components of IMF (from *Wind*); simultaneous changes of A_{He} and the proton density, N (b) and thermal velocity, V_{th} (c). In these figures, A_{He} is plotted in red and other parameters, N (in (b)) and V_{th} (in (c)) in blue, respectively.

(A color version of this figure is available in the online journal.)

these two lines reveals abrupt changes of A_{He} that are quantified in the third panel. Consistent with the low solar wind speed ($\approx$320 km s^{-1}), the time interval starts with $A_{\mathrm{He}} \approx 1\%$. The most impressive A_{He} jump (by a factor of five) at $\approx$0751 UT correlates with the drop of the proton density by a factor of 3.5 and with the slight drop of the proton thermal speed. However, many other step-like changes of A_{He} are not accompanied by changes of other quantities. The IMF propagated from *Wind* in the bottom panels shows that while the A_{He} jump at $\approx$0751 UT likely occurs simultaneously with a large IMF rotation, none of the other A_{He} jumps can be associated with IMF changes. Another interesting feature is that the solar wind speed was low and nearly constant across the whole interval except for the jumps of all parameters at $\approx$0824 UT where the speed rises from 320 to 330 km s^{-1}.

The detailed plots of the A_{He} jump at 0751 UT in Figures 3(b) and (c) demonstrate that it occurred within 9 s of changes of the thermal speed, V_{th}, and proton density, N. The duration of

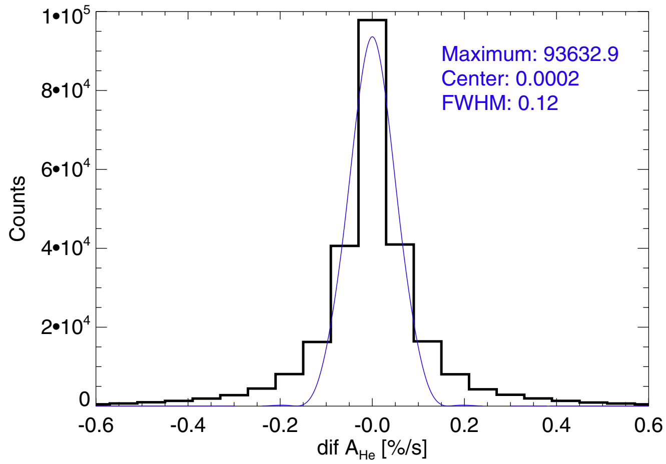

Figure 4. Distribution of derivatives of $A_{\rm He}$.
(A color version of this figure is available in the online journal.)

the jump and the solar wind speed provide the thickness of the transition layer of about 3000 km, i.e., only several alpha thermal gyroradii. Despite the constant solar wind speed, we believe that this jump can be attributed to the crossing of the flux tube wall.

In order to find how frequent such abrupt variations are, we have computed distributions of $\mathrm{dif}A\mathrm{He} = dA_{\rm He}/dt$ as the difference of two consecutive $A_{\rm He}$ measurements divided by the time between them and plotted the results in Figure 4. A comparison of this distribution with the Gaussian fit shown as the thin line suggests a strongly enhanced probability of steep jumps of $A_{\rm He}$ in both directions. The same is true for changes of the proton density, speed, and temperature (not shown). These results agree with a similar analysis in Owens et al. (2011).

Since abrupt changes of $A_{\rm He}$ are usually attributed to crossings of the boundaries between solar wind streams emanating from different source regions in the solar corona or boundaries of flux tubes, one would expect that these changes would be accompanied by corresponding variations of the other parameters, similar to the event analyzed in Figures 3(b) and (c).

To check this idea, Figure 5 presents two-dimensional histograms of the probability of simultaneous observations of steep changes of $A_{\rm He}$ and of the changes of one of proton moments defined analogous. The three top panels show jumps computed from 30 s averages, whereas the full resolution ($\approx$3 s) data are used in bottom panels. We show the full resolution and averaged data because the duration of significant $A_{\rm He}$ jumps is often larger than 3 s; thus, the same jump can be represented by several points if the full resolution is applied. This effect disappears in the averaged data. The color scale represents a number of events in a particular bin. In order to show the probabilities of observations of steep changes, we have limited the color scale to 1000. The white bins with larger counts concentrated at the center of the panels indicate that "no change" is the preferred state of quantities on both axes. The values of derivatives of all parameters are an order of magnitude lower in the top panels than those in bottom (compare the scales), which indicates a prevalence of short and sharp jumps that are smoothed in averaged data. On the other hand, the patterns important for the data interpretation are the same and they are clearly visible in both sets. Presuming the association of changes of $A_{\rm He}$ with crossings of the flux tube boundaries, one would expect distinct diagonal patterns in

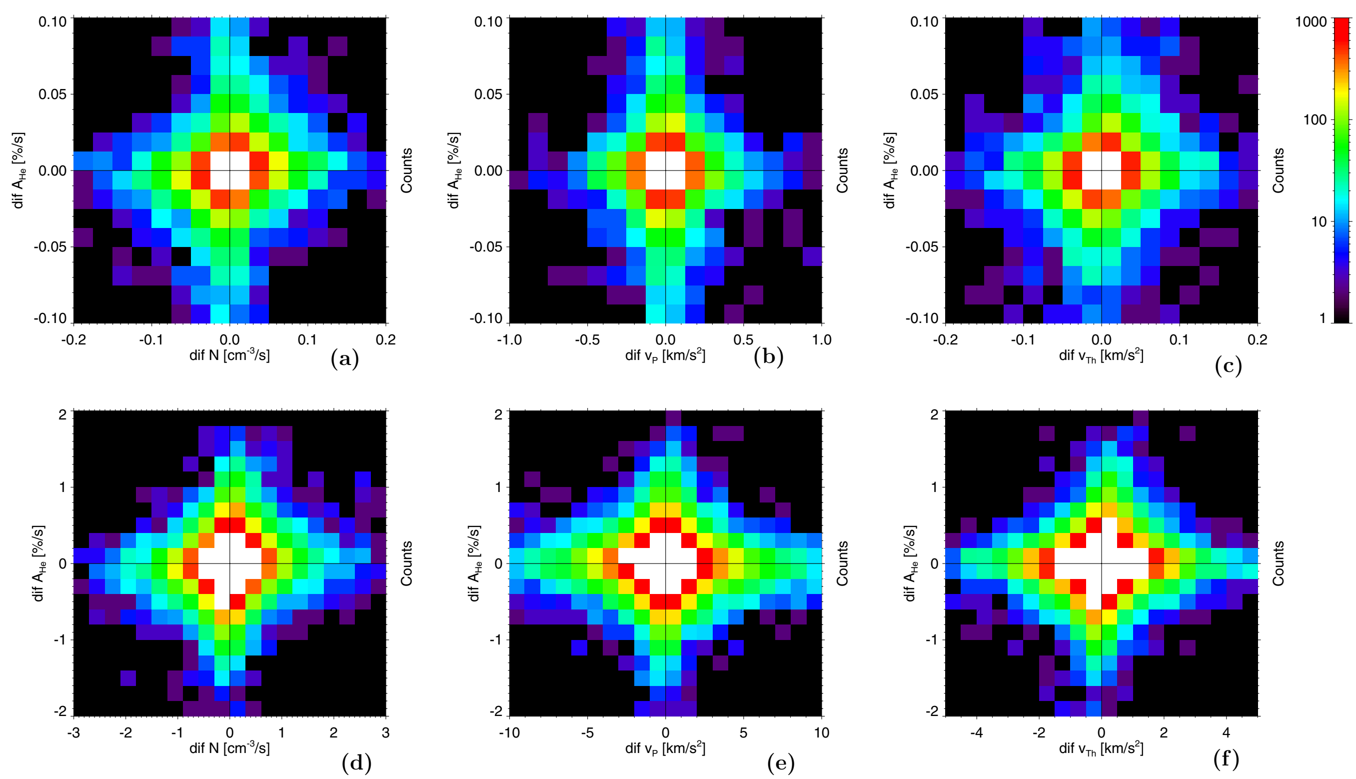

Figure 5. Derivative of $A_{\rm He}$ versus derivatives of other parameters—30 s averages (panels (a), (b), and (c)) and the same derivatives of parameters with a full resolution (panels (d), (e), and (f)). The color scales represent a number of observed events. The parameters in particular panels are (a) and (d) densities; (b) and (e) bulk speeds; and (c) and (f) thermal speeds.

(A color version of this figure is available in the online journal.)

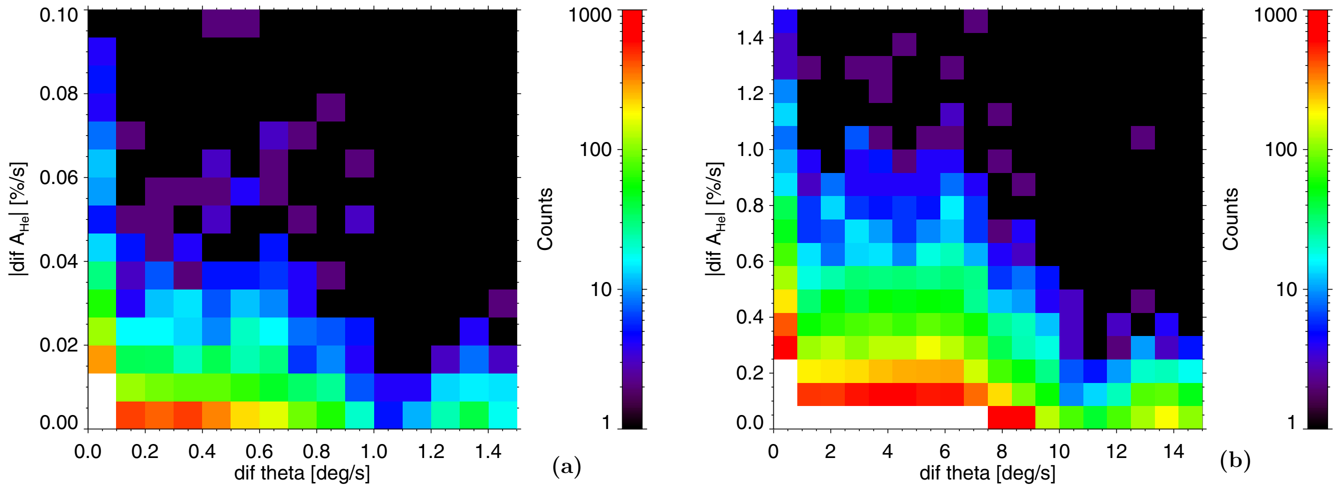

Figure 6. Derivative of A_{He} as a function of derivative of the solar wind flow cone angle, θ - 30 s averages (panel (a)), and the same derivatives for a full resolution (panel (b)). The color scales represent a number of observed events.

(A color version of this figure is available in the online journal.)

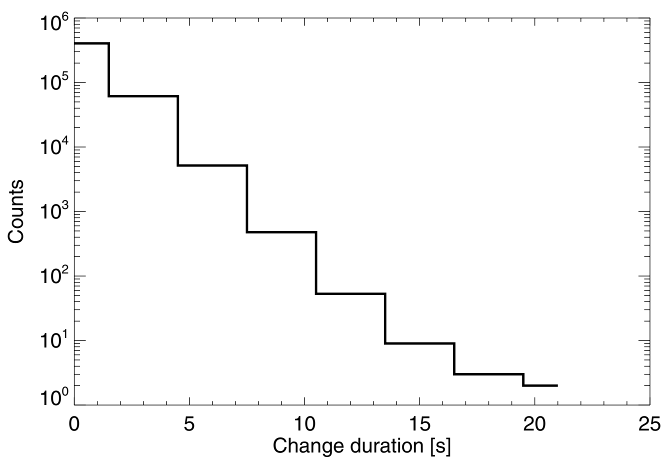

Figure 7. Duration of continuous increase/decrease of A_{He}.

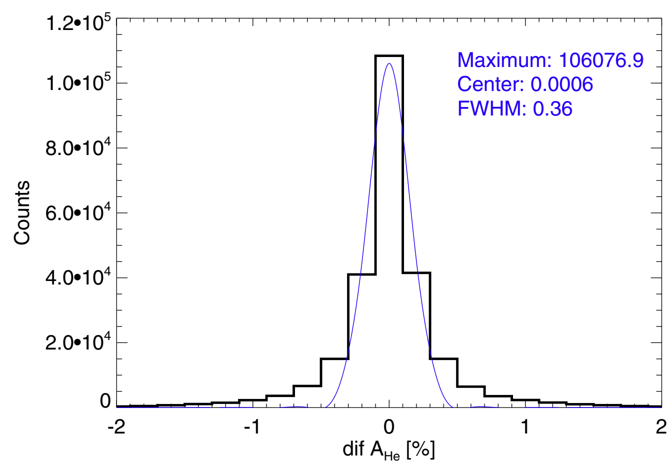

Figure 8. Distribution of A_{He} jump magnitudes.

(A color version of this figure is available in the online journal.)

Figure 5. However, the largest numbers of events are concentrated along the axes and it indicates that abrupt variations of A_{He} are generally uncorrelated with changes of other quantities and vice versa.

A very weak positive correlation of A_{He} variations with the density and temperature jumps can be seen in both averaged and full resolution data, but there is no relation of the variations in A_{He} and in the proton speed. The connection between A_{He} changes and fluctuations of the solar wind velocity direction is analyzed in Figure 6. The presentation is similar to that in Figure 5. The data are binned according to the change of the cone angle (the angle between the solar wind velocity and sunward direction, θ). Due to the lack of magnetic field measurements, we cannot analyze variations of the magnetic field that are believed to occur at the walls between flux tubes of different origins, but we believe that the changes of the solar wind direction would be a suitable indicator of the crossings of such boundaries. Nevertheless, neither the averaged plot (Figure 6(a)) nor the full resolution data (Figure 6(b)) exhibit a significantly better organization than the plots in Figure 5. Several blue points near the diagonal in Figure 6(a) probably result from crossings of the stream boundaries like that shown in Figure 3, but most events are again concentrated along the axes. This result is surprising because the bulk speed is usually taken as a typical characteristic of a particular flux tube. For example, Borovsky (2008) found 40.6 km s^{-1} as the median velocity difference between neighboring tubes.

Figures 4–6 discuss the changes of A_{He} and simultaneous changes of other plasma parameters on 3 s intervals. Large fronts with a duration >3 s are represented by several events in these figures. This analysis shows the large overall variability of the investigated quantities, but the analysis made on fixed time intervals cannot determine whether the observed changes are connected with the crossings of flux tube boundaries or if they originate from another source(s).

For this reason, we have prepared an additional study that examines front durations and their magnitudes. Figure 7 shows the distribution of the duration of the fronts of abrupt A_{He} changes. The duration is defined as a number of consecutive intervals within which A_{He} increases (or decreases) continuously more than 0.1% s^{-1}. One can note a nearly exponential decrease of the number of observed fronts with their duration. The increase of the front duration by one time step (3 s) leads to a decrease of the number of the found fronts by an order of magnitude.

Figure 8 presents the distribution of the front heights. One would expect that the steepness of the fronts would be correlated with their heights and, indeed, the distribution is very similar to that shown in Figure 4. In addition to the random changes of A_{He} that can be described by the Gaussian fit, there is a non-negligible portion of large jumps. Moreover, the jumps were chosen by an automated routine that expects a continual increase (decrease) of A_{He} within the front. If there were a glitch inside the front like that in Figure 3(b), the front height would be underestimated in a comparison with the height that would be identified, for example, by an inspection of individual plots.

4. DISCUSSION AND CONCLUSION

The paper analyzes variations of a relative He abundance in the solar wind that were determined from measurements of ion energy spectra by the BMSW instrument on board the *Spektr-R* spacecraft (Šafránková et al. 2013c). The analysis is focused on timescales from seconds to tens of seconds. Since the He/H ratio was determined as a ratio of FC currents corresponding to protons and alpha particles, our A_{He} ratio refers to fluxes of particles rather than the density ratios that were used in the studies mentioned in the Introduction. Our results can be compared with previous results only if H and He are assumed to have the same speed. The differential flow does not exceed 30 km s^{-1} at Earth's orbit (Neugebauer et al. 1996) and thus the assumption of equal speeds would result in an uncertainty lower than 10%. This uncertainty does not spoil our interpretation of the results because we are studying variations much stronger than 10%.

Since the data cover one year at the ascending phase of the solar cycle, one can expect that A_{He} would be a rising function of the solar wind speed and would vary between 1%–5% in accord with the corresponding solar wind stream (Kasper et al. 2007). Our statistics shows that the averaging used in previous papers does not reveal the full range of A_{He} variations because we have found a significant (≈5%) probability of observations of larger (>8%) A_{He} values and several short intervals with $A_{\mathrm{He}} > 10\%$. These values were observed in a cold solar wind at speeds above 500 km s^{-1} (see Figures 2(a) and (c)), in contrast with the general trend of increasing A_{He} with the proton thermal speed (Figure 2(c)). This increase could be a consequence of the well known fact that both the solar wind temperature and A_{He} are rising functions of the solar wind speed. However, another possible interpretation is that the higher proton temperature of the fast solar wind can result from enhanced He content that leads to excitation of waves which in turn heat the protons. The connection between wave activity and A_{He} can be inferred from Figures 2 and 3 of the Bourouaine et al. (2011) paper. The energy source for this heating would be the difference between the speeds of the ion species that decreases with the traveled distance (Marsch et al. 1982; Neugebauer et al. 1996). This suggestion is consistent with well known facts that the He abundance as well as the difference of velocities of these species are larger in the fast solar wind. A simple quantitative estimate shows that 30 km s^{-1} of difference between proton and alpha speeds represents enough free energy to heat the whole ion population by ≈5 eV per 1% of A_{He}. Aforementioned extreme A_{He} values that contradict the general trend of the proton thermal speed increase with A_{He} should be further investigated. A possible candidate is an encounter of interplanetary coronal mass ejections (Yermolaev & Stupin 1997).

The principal feature of this study is the presentation of high-time resolution measurements that reveal large A_{He} variations that could not be observed in previous studies using one minute data resolution. Figure 4 shows a significant portion of the events

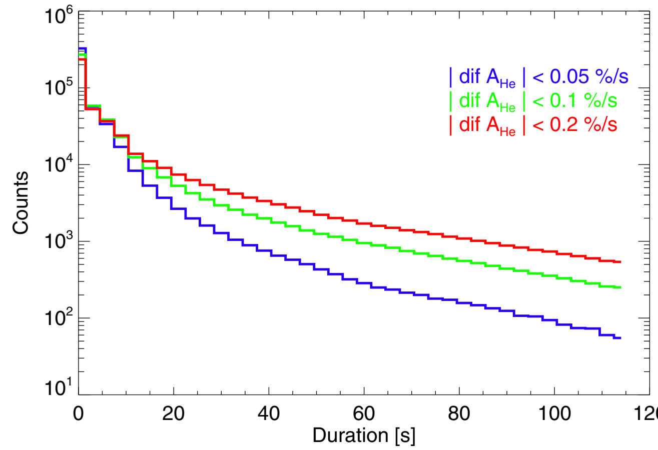

Figure 9. Distribution of quiet interval durations (see the text for definition). (A color version of this figure is available in the online journal.)

have a change rate exceeding 0.2% A_{He} s^{-1}. We believe that an increase of the time resolution would identify even steeper changes resulting from kinetic effects. A careful examination of the A_{He} fast fluctuations presented in Figures 5 and 6 shows that the A_{He} jumps are not correlated with variations of the proton velocity magnitude (Figures 5(a) and (d)), direction (Figure 6), or with variations of the other investigated parameters. The analysis of durations and heights of the A_{He} jumps presented in Figures 7 and 8 indicated that only 10% of the observed jumps last longer than one our time step (≈3 s) and only a negligible number (<0.5%) has longer than 10 s. This result does not correspond to the generally accepted interpretation of A_{He} changes as resulting from crossings of solar wind flux tubes from different source regions. The streams with low He abundance emanate from the streamer belt, whereas the He-enriched streams originate at boundaries of coronal holes. These streams would generally have different speeds and/or other parameters, but A_{He} would be about constant within a particular stream. However, the low/high-speed streams are usually large and long-lived structures that cannot be differentiated properly in our data set due to its limitation to speeds below 600 km s^{-1}. Borovsky (2008) suggested that the fine solar wind structure is composed of flux tubes bounded by jumps of the magnetic field and plasma parameters (including A_{He}), but that the variations of these parameters inside a particular flux tube would be low.

In order to examine the consistency of this structure with the data, we searched for intervals with small variations of A_{He}. Figure 9 presents the results of this search for three levels of variations. The red line shows the distribution of durations of intervals within which the slope of the A_{He} change did not exceed 0.2% s^{-1}. Since our time step is about 3 s, it means that the A_{He} difference measured at two neighboring points was lower than ≈0.6%. The figure reveals that the duration of about 80% of intervals is 3 s, i.e., one our time step, and that only about 0.5% of quiet intervals are longer than 100 s. The other two profiles shown in Figure 9 demonstrate that a more restrictive definition of the quiet interval leads to a further significant decrease of their length.

The median cross-section of the solar wind flux tubes at 1 AU is ≈4.4 × 10^5 km (Borovsky 2008 and references therein). A spacecraft should thus spend about ≈1000 s in one particular tube, but our results in Figure 9 show that the typical time between abrupt changes of A_{He} is much shorter.

Taking Figure 3(a) as an example, the first abrupt change of A_{He} can probably be attributed to a crossing of the flux tube boundary in spite of a negligible change of the speed. The variations observed in the rest of the depicted interval are large and often step functions but are too frequent to be attributed to different coronal sources because the duration of the whole depicted interval roughly corresponds to two typical cross-sections of solar wind flux tubes. Moreover, the analyzed data set covers ≈180 hr of measurements and thus only about 700 crossings of flux tube boundaries should be observed; in our data set, such boundaries cannot be distinguished from the plethora of other changes.

A natural explanation of these features and the presented statistical results is that a majority of observed A_{He} variations is generated by turbulence. A slight correlation of these jumps with proton density and temperature variations indirectly supports this interpretation.

Borovsky (2008) discusses four possible sources of the origin of flux tubes in the solar wind on its path from the Sun to 1 AU; namely, (1) spontaneous formation of the thin current sheets, (2) MHD turbulence, (3) non-linear steepening of outward traveling Alfvén waves, and (4) formation of mesoscale zonal flows due to the drift turbulence. His main argument against all of these sources is that none can lead to changes of the ion composition that are frequently observed across flux tube boundaries. However, our study of the changes of the relative He abundance has shown that such changes are frequent and even very abrupt transitions of the ion composition occur without notable variations of other plasma parameters (Figures 5 and 6). Figure 9 demonstrated that a typical duration of intervals with approximately constant A_{He} is of the order of seconds. The projection of such tiny structures toward the solar corona would lead to dimensions comparable with the ion gyroradius.

As noted above, we suggest that the turbulence driven by the proton-alpha differential flow is able to create the observed fast changes of A_{He}. Such features are not observed in standard MHD models because only one ion component is usually considered and either full particle or hybrid codes with two species like that used in Perrone et al. (2011) should be applied.

Finally, we stress that data showing the changes of A_{He} on short (3–30 s) time scales from which we derived our statistics were not previously available. We suggest that these variations are generated by the turbulence driven by the H–He differential flow. This hypothesis does not contradict the generally accepted interpretation of A_{He} jumps observed on larger (minutes to hours) scales as remnants of the structure of solar wind coronal sources.

The present work was partly supported by the Czech Grant Agency under contracts P209/12/1774 and 205/09/0170, and partly by the Research Plan MSM 0021620860, which is financed by the Ministry of Education of the Czech Republic.

Facility: SRT

REFERENCES

Aellig, M. R., Lazarus, A. J., & Steinberg, J. T. 2001, GeoRL, 28, 2767

Avanov, L., Borodkova, N., Němeček, Z., et al. 1987, CzJPh, 37, 759

Bame, S. J., Asbridge, J. R., Feldman, W. C., & Gosling, J. T. 1977, JGR, 82, 1487

Borovsky, J. E. 2008, JGR, 113, 8110

Borrini, G., Wilcox, J. M., Gosling, J. T., Bame, S. J., & Feldman, W. C. 1981, JGR, 86, 4565

Bourouaine, S., Marsch, E., Neubauer, F. M., & Fritz, M. 2011, ApJL, 728, L1

Feldman, W. C., Asbridge, J. R., Bame, S. J., & Gosling, J. T. 1978, JGR, 83, 2177

Kasper, J. C., Lazarus, A. J., & Gary, S. P. 2008, PhRvL, 101, 261103

Kasper, J. C., Stevens, M. L., Lazarus, A. J., Steinberg, J. T., & Ogilvie, K. W. 2007, ApJ, 660, 901

Marsch, E., Muhlhauser, K. H., Rosenbauer, H., Schwenn, R., & Neubauer, F. M. 1982, JGR, 87, 35

Neugebauer, M. 1981, FCPh, 7, 131

Neugebauer, M., Goldstein, B. E., Smith, E. J., & Feldman, W. C. 1996, JGR, 101, 17047

Ogilvie, K. W., Coplan, M. A., Bochsler, P., & Geiss, J. 1989, SoPh, 124, 167

Ogilvie, K. W., & Hirshberg, J. 1974, JGR, 79, 4595

Owens, M. J., Wicks, R. T., & Horbury, T. S. 2011, SoPh, 269, 411

Perrone, D., Valentini, F., & Veltri, P. 2011, ApJ, 741, 43

Richardson, J. D., & Kasper, J. C. 2008, JASTP, 70, 219

Šafránková, J., Němeček, Z., Přech, L., & Zastenker, G. N. 2013a, PhRvL, 110, 025004

Šafránková, J., Němeček, Z., Přech, L., & Zastenker, G. N. 2013b, in AIP Conf. Proc. 1539, Fast Solar Wind Monitoring Available: BMSW in Operation (Melville, NY: AIP), 466

Šafránková, J., Němeček, Z., Přech, L., et al. 2013c, SSRv, 175, 165

Steinberg, J. T., Lazarus, A. J., Ogilvie, K. W., Lepping, R., & Byrnes, J. 1996, GeoRL, 23, 1183

Viall, N. M., Spence, H. E., & Kasper, J. 2009, GeoRL, 36, 23102

Wang, Y.-M. 2008, ApJ, 683, 499

Yermolaev, Y. I., & Stupin, V. V. 1997, JGR, 102, 2125